Articles in PresS. Am J Physiol Lung Cell Mol Physiol (June 17, 2005). doi:10.1152/ajplung.00069.2005

"FINAL ACCEPTED VERSION"

CYCLIC MECHANICAL STRAIN INCREASES REACTIVE OXYGEN SPECIES PRODUCTION IN PULMONARY EPITHELIAL CELLS

Kenneth E. Chapman[1], Scott E. Sinclair[3], Daming Zhuang[2], Aviv Hassid[2], Leena Desai[2], and Christopher M. Waters[2]

Department of Biomedical Engineering[1]

Northwestern University, Evantson, IL 60208

And Departments of Physiology[2] and Medicine[3]

The University of Tennessee Health Science Center

Memphis, TN 38163

Address correspondence to:

Christopher M. Waters, Ph.D.

Department of Physiology

The University of Tennessee Health Science Center

894 Union Ave, Room 426

Memphis, TN 38163-0001

Phone: (901) 448-5799

Fax: (901) 448-7126

Email: cwaters@physio1.utmem.edu

Running Title: Strain increases ROS production in PEC

Key words: mechanotransduction, ventilator induced lung injury

Support: NIH grants HL064981, HL004479, HL63886, and HL72902

ABSTRACT

Over-distention of lung tissue during mechanical ventilation may be one of the factors that initiates ventilator-induced lung injury (VILI). We hypothesized that cyclic mechanical stretch (CMS) of the lung epithelium is involved in the early events of VILI through the production of ROS. Cultures of an immortalized human airway epithelial cell line (16HBE), a human alveolar type II cell line (A549), and primary cultures of rat alveolar type II cells (AT II) were cyclically stretched, and the production of superoxide (O_2^-) was measured by dihydroethidium fluorescence. CMS stimulated increased production of O_2^- after 2 h in each type of cell. 16HBE cells exhibited no significant stimulation of ROS before 2 h CMS (20% strain, 30 cycles/min), and ROS production returned to control levels after 24 h. Oxidation of glutathione (GSH), a cellular antioxidant, increased with CMS as measured by a decrease in the ratio of the reduced GSH level to the oxidized GSH level. Strain levels of 10% did not increase O_2^- production in 16HBE cells whereas 15, 20, and 30% significantly increased generation of O_2^-. Rotenone, a mitochondrial Complex I inhibitor, partially abrogated the stretch-induced generation of O_2^- after 2 h CMS in 16HBE cells. NADPH oxidase activity was increased after 2 h of CMS contributing to the production of O_2^-. Increased ROS production in lung epithelial cells in response to elevated stretch may contribute to the onset of VILI.

INTRODUCTION

In patients with acute hypoxemic respiratory failure, mechanical ventilation strategies employed to improve arterial oxygenation can initiate or exacerbate lung injury. Mechanisms implicated in ventilator-induced lung injury (VILI) include high inspiratory volumes or "volutrauma," mechanical stress-induced inflammation or "biotrauma", and cyclical airway collapse and reopening. Low tidal volume ventilation strategies that minimize over-distention of the lung tissue decrease mortality in patients with acute respiratory distress syndrome (ARDS) presumably by limiting or preventing additional VILI (40). Recent animal studies in a mouse model of VILI demonstrated that high tidal volume ventilation without underlying lung injury led to increased neutrophil infiltration (5) and pro-inflammatory cytokines in the lungs (46) indicating a link between volutrauma and biotrauma. However, the factors leading from mechanical stress to the initiation and propagation of VILI remain uncertain. One potential initiating signal may be increased production of reactive oxygen species (ROS) in the lung epithelium in response to increased stretch.

Increased ROS production in response to mechanical stress has been described in a variety of cell types. Endothelial cell production of ROS has been shown to increase in response to shear stress (4, 6, 7, 10, 19, 30, 45, 50) and to cyclic mechanical stretch (CMS) (2, 29, 47, 48). CMS also stimulates ROS production in vascular smooth muscle cells (13, 22, 31) and cardiac myocytes (1). Although superoxide (O_2^-) appears to be the initial species generated in these cell types, there is disagreement as to the source of ROS production. The NADPH oxidase system (7, 13, 29, 30), mitochondrial production (2, 21), and the xanthine oxidase system (30) have all been implicated as potential sources

for increased superoxide production in response to mechanical stress. However, whether these potential sources are activated directly or indirectly by mechanical stress is unclear. Little data are available demonstrating increased ROS production by stretched alveolar or airway epithelial cells. A 25% increase in ROS production, as measured by DCFH fluorescence caused by interaction with hydrogen peroxide (H_2O_2), was measured in response to 30% biaxial stretch of A549 cells, a human alveolar Type II-like cell line (42). In another study A549 cells subjected to cyclic stretch produced significantly increased levels of isoprostane (a marker of oxidant injury) after 0.5 h, and levels of reduced glutathione (GSH, an endogenous antioxidant) were significantly decreased after 1 h of CMS (23). Pretreatment with antioxidants prevented the change in isoprostane levels in this study. However, the source(s) of increased ROS production and species generated in pulmonary epithelial cells exposed to mechanical stretch have not been determined.

In the current study, we examined whether cyclic mechanical strain induced production of O_2^- in the main epithelial constituents of the lungs, airway (AEC) and alveolar (AlvEC) epithelial cells. Superoxide production was significantly enhanced in an SV40-transformed human AEC line (16HBE), A549 cells, and isolated primary rat alveolar type II (rat AT II) epithelial cells undergoing CMS. Increased ROS production was dependent upon the time and magnitude of stretch. The source of the O_2^- was a combination of the NADPH oxidase system and the mitochondria (Complex I). Mitochondrial involvement may be initiated by a direct distention of the mitochondria due to mechanical stretch.

MATERIALS AND METHODS

Reagents. Unless otherwise noted, all chemicals were purchased from Sigma-Aldrich Chemical Company (St. Louis, MO).

Cell Culture. 16HBE cells were generously provided by Dr. Deiter Gruenert, and were cultured in DMEM (Gibco, Carlsbad, CA) with 4 mM glutamine supplemented with 10% fetal bovine serum (FBS) (Cellgro, Herndon, VA or Gibco, Carlsbad, CA), 20 mM HEPES (Sigma, St. Louis, MO), and 2.5 μM Plasmocin (Invivogen, San Diego, CA). These cells were first treated for 2 weeks with 25 μg Plasmocin. A549 cells were cultured in DMEM with 4 mM glutamine supplemented with 10% fetal bovine serum (FBS) (Cellgro) and 1% penicillin/streptomycin solution (Gibco). Both cell types were cultured until 85-100% confluence before being seeded onto the BioFlex plates coated with collagen type I (Flexcell International, Inc., Hillsborough, NC) for studies on confluent monolayers. The medium was changed every other day for all cultures.

Isolation and Culture of Rat Alveolar Type II Cells. Primary rat AT II cells were isolated according to established procedures (8, 26, 32). Briefly, male Sprague-Dawley rats were anesthetized with phenobarbital, killed by exsanguination, and their lungs were excised. The trachea was catheterized and the pulmonary vasculature perfused via the pulmonary artery with solution II (140 mM NaCl , 5 mM KCl, 2.5 mM Na_2HPO_4, 10 mM HEPES, 1.3 mM $MgSO_4$, and 2.0 mM $CaCl_2$; pH 7.4) to remove the blood. The airspaces were then lavaged with Solution I (140 mM NaCl , 5 mM KCl, 2.5 mM Na_2HPO_4, 6 mM glucose, 0.2 mM EGTA, and 10 mM HEPES; pH 7.4) to remove free, non-epithelial cells. Elastase (4.3 units/ml in Solution II; Worthington Biochemical Corporation, Lakewood, NJ) was instilled in the airspace and incubated at 37° C for 10

min. This was repeated and the large airways and heart were removed. The remaining lung tissue was then minced in 5 ml of FBS and 250 μl of 250 μg/ml DNAse (Sigma) per 4 lungs. The minced lungs were filtered through gauze followed by a nitrocellulose membrane, and the cell suspension was collected. The suspension was centrifuged and resuspended in AT II culture medium [DMEM with 10% heat-inactivated FBS (HyClone, Logan, UT), 4 mM glutamine, 1% pen/strep, and 0.25 μM amphotericin B (Sigma)] and plated on untreated petri dishes coated with IgG. The plates were incubated for 1 h to allow non-epithelial cells such as macrophages to bind to the IgG. The plates were "panned" to loosen non-specifically bound cells, pooled, and counted. BioFlex plates coated with collagen type I by the manufacturer were then coated with 32.3 μg/ml human fibronectin (Roche Life Sciences, Indianapolis, IN), and cells were seeded to confluence at 3.0 x 10^6/well in AT II culture medium. Experiments were performed on Day 2 after isolation. AT II cells were identified using Nile Red (Sigma) staining of lamellar bodies, and >90% of the cells were Nile Red positive on day 2.

Application of Mechanical Strain. Strain was applied using a Flexercell strain unit 4000 (Flexcell International, Inc.), a vacuum driven device that applies biaxial strain to cells cultured on Silastic-bottomed well plates. The device allows control of the frequency of strain and magnitude up to 30% linear strain. 16HBE and A549 cells were strained at 20% elongation and 30 cycles per minutes (cpm) for the initial studies. This strain profile was previously found to maximally inhibit wound closure in AEC cells (38). Rat AT II cells were strained at 15% elongation and 15 cpm because higher levels of strain and frequency resulted in increased cell detachment from the culture plate.

Mearsurement of Superoxide Production. Intracellular O_2^- production was measured by the fluorescent intensity of oxoethidium after dihydroethidium (Molecular Probes, Eugene, OR) was oxidized by O_2^-. Oxoethidium binds to DNA becoming highly fluorescent. After treatment, cells were rinsed 2x with warm serum- and phenol red-free (PR-Free) DMEM and loaded with 5 μM DHE in PR-Free DMEM at 37° C in the incubator for 30 min. The cells were then rinsed once with room temperature PR-Free DMEM, fresh PR-Free DMEM at room temperature was added, and the cells were imaged immediately. Images were taken on an inverted fluorescent microscope (TE300, Nikon Instuments, Lewisville, TX) outfitted with a 20x PlanFluor objective (Nikon Instruments), rhodamine filter set for excitation and emission (Chrorma Technology Corp., Rockingham, VT), and digital CCD camera (Roper Scientific, Tucson, AZ). Images were acquired using MetaMorph software (Universal Imaging, Downingtown, PA) for 10 s with a 4x ND filter engaged. Four separate images were taken per well avoiding areas of low confluence and areas near the edge of the well. The average pixel intensity per image was calculated and an average intensity per well was determined. To assess the involvement of the mitochondria, treatment with the pharmacological inhibitor of the mitochondrial Complex I, rotenone (25 nM), was initiated at the beginning of the stretch protocol.

Measurement of Reduced and Oxidized Glutathione Levels. A protocol from Kamencic et al. (25) adapted for a fluorescent plate reader was used to determine levels of reduced and oxidized GSH. 16HBE cells were stretched or held static for various periods of time and then placed on ice. The cells were rinsed twice with ice cold Ca^{2+}/Mg^{2+} free DPBS. Ice-cold cell lysate buffer (0.5 ml, 0.2 mM

ethylenediaminetetraacetic acid (EDTA) in Ca^{2+}/Mg^{2+} free DPBS) was added to each well. The cells were scraped and transferred to centrifuge tubes at 4° C. Samples were sonicated on ice for 20 s. The samples were centrifuged for 10 min at 10,000 x g and 4° C. Two 100 μl aliquots of each sample were diluted with 200 μl of de-ionized H_2O per aliquot. One diluted aliquot from each sample was completely reduced by the addition of 15 μl of 4 M triethanolamine (TEA) to determine the total amount of GSH. A standard curve of GSH with and without TEA was created. Wells of a black 96-well plate were loaded with 50 μl of diluted sample and 150 μl of assay solution (100 μM monochlorobimane, 1 U/ml glutathione-S-transferase, 0.2 mM EDTA in Ca^{2+}/Mg^{2+} free DPBS), and the plate was incubated in the dark for 30 min at room temperature. The plate was then read in a fluorescence plate reader (Molecular Devices, Sunnyvale, CA) with excitation at 380 nm and emission at 470 nm. To calculate the oxidized GSH (GSSG), the amount of reduced GSH was subtracted from the TEA treated sample and divided by two to account for the dimerization. The ratio of reduced GSH/GSSG was then calculated to monitor the redox state of the cells.

NADPH Oxidase Assay. The assay used to determine NADPH oxidase activity was adapted from previous studies (7, 51). Cells were stretched or held static, placed on ice, and rinsed 3 times in ice cold DPBS. Cells were placed in 0.5 ml of homogenization buffer [1 mM ethylene glycol-bis(2-aminoethylether)-*N,N,N′,N′*-tetraacetic acid (EGTA), 10 μg/ml aprotinin, 0.5 μg/ml leupeptin, and 0.5 mM phenylmethanesulfonyl fluoride (PMSF) in Ca^{2+}/Mg^{2+} free DPBS], scraped, homogenized manually, and placed in tubes. Cell homogenate (50 μl) was added to 3 ml of warm chemiluminescence buffer (10 μM Lucigenin, 1 mM EGTA and 150 mM sucrose in Ca^{2+}/Mg^{2+} free DPBS)

containing NADPH (50 μM) in a scintillation vial. Chemiluminescence was measured (in duplicate) for 3 min in a Packard scintillation counter. Diphenylene iodonium (DPI, 10 μM) was included in the chemiluminescence buffer for selected static and stretched samples.

Staining and Imaging of Mitochondria of Stretched Cells. 16HBE cells were cultured on collagen I-coated Silastic membranes for the StageFlexer (Flexcell International, Inc.), which is a single membrane stretching device adapted for use on a microscope stage. Live 16HBE cells were stained with 500 nM MitoTracker Orange (Molecular Probes) for 30 min and rinsed twice with warm DPBS. Membranes were placed in the StageFlexer and images were acquired with a 60x objective (Nikon) before and after the application of ~17% biaxial strain. Since images included contributions of structures from multiple planes, we selected structures that were likely to be in thin or confined regions of the cells such as beneath the nucleus and near the edges of the cells. The total length of each mitochondrion was measured by tracing a line down the centerline of each structure to determine the overall length before and during strain.

Statistical Analysis. All values are presented as mean ± standard error (SE). All statistical analyses were performed with the SigmaStat statistical package (Version 2.03, Jandel Scientific, San Rafael, CA). One-way ANOVA was performed for comparisons of multiple treatments. If this showed significant difference between the treatments, a Student's t-test with the Bonferroni correction was performed to determine significant differences between the individual conditions. All of the ANOVA tests were run with multiple comparisons against the static control except for the data collected using the mitochondrial inhibitor, rotenone. These experiments employed multiple comparisons

between all of the different treatments. Significant differences are based on a threshold of $p \leq 0.05$.

RESULTS

Cyclic mechanical stretch (CMS) induces superoxide (O_2^-) production in pulmonary epithelial cells. To determine if CMS increased O_2^- production in AEC and AlvEC, we subjected 16HBE cells, A549 cells, and primary rat AT II cells to 2 h of CMS and measured the O_2^- production via DHE fluorescence. Figure 1A shows a region of representative images of 16HBE cells showing the changes in DHE fluorescence intensity following 2 h of CMS. Superoxide production was significantly increased in each of the cell types that we tested compared with static controls (see Figure 1B). The A549 cells exhibited the strongest response to CMS (142.5 ± 0.5%; $p < 0.05$, $n = 3$) after 2 h of stretch, but 16HBE and rat AT II cells displayed the same order of magnitude increase in O_2^- production (126.7 ± 1.9% and 114.9 ± 2.8%; $p < 0.05$, $n = 9$ and 6, respectively). However, rat ATII cells were stretched at a lower frequency and magnitude due to cell detachment at the higher levels.

Time course of O_2^- production in response to stretch. We further investigated the time-course of O_2^- production in 16HBE cells in response to CMS. Figure 2 shows that there was no significant change after 0.5 h of stretch, but the O_2^- production increased significantly after 2 h, achieving the maximal response after 6 h (157.2 ± 9.2%; $p < 0.05$, $n = 9$), and remained significantly elevated up to 18 h (118.4 ± 5.4%; $p < 0.05$, $n = 9$) before returning to baseline after 24 h. These results suggest an initial increase in O_2^- production in response to the initiation of stretch followed by a later adaptation to increased O_2^- production.

Oxidation of glutathione (GSH) increased in 16HBE cells exposed to CMS. To determine whether the measured superoxide production was increased due to a change in

the redox state of the cells, we measured the relative levels of oxidized (GSSG) and reduced (GSH) glutathione. Reduced glutathione is an important cellular defense against ROS that forms a dimer with a disulfide bond (GSSG) upon oxidation. The ratio of GSH/GSSG is a marker of the redox state of the cell and is reduced when the cells experience an oxidative stress. We measured this ratio to determine if the ROS generated by CMS caused changes in the redox state of 16HBE cells. Figure 3 shows that 0.5 h of CMS caused a significant reduction in the normalized GSH/GSSG ratio to 50.8 ± 4.4 % of the 0 h control ($p < 0.05$, $n = 4$) indicating a persistent oxidative stress. The GSH/GSSG ratio remained significantly reduced through 24 h reaching 40.5 ± 7.5 of control at its lowest point after 24 h of CMS. Thus, although O_2^- production had returned to control levels after 24 h of CMS (Figure 2), the ratio of GSH/GSSG remained significantly reduced.

Superoxide production is dependent upon the magnitude of CMS. To determine whether increased O_2^- production was dependent on the magnitude of CMS, 16HBE cells were stretched for 2 h at 10, 15, 20, and 30% strain and the O_2^- production was measured by DHE fluorescence. Figure 4 shows that 10% CMS did not significantly increase O_2^- production, but levels of strain 15% and higher resulted in significant increases after 2 h of strain.

Mitochondrially derived O_2^- is partially responsible for cyclic mechanical strain-induced production of O_2^-. Mitochondria are the largest source of intracellular ROS production from normal cell respiration, and have been implicated in ROS production stimulated by mechanical deformation of endothelial cells (2, 21). To investigate whether stretch-induced O_2^- production was due to increased mitochondrial generation,

we treated 16HBE cells with the Complex I inhibitor, rotenone. As shown in Figure 5, rotenone (25 μM) partially but significantly inhibited the enhanced O_2^- production after 2 h of CMS from 143.7 ± 4.8% to 120.7 ± 2.5% ($p < 0.05$, $n = 6$), but the response was still significantly greater than control ($p < 0.05$, $n = 6$). Cells treated with the vehicle used to solubilize the rotenone (chloroform) demonstrated a response similar to that of untreated controls after 2 h of CMS (138.2 ± 6.6%, $p < 0.05$, $n = 3$). These results suggest that at least part of the increased O_2^- production was generated by the mitochondria.

Mitochondria are deformed by mechanical strain. Although increased mitochondrial production of superoxide has been previously reported in endothelial cells (2, 21), the mechanism of stimulation is not known. To investigate whether increased mitochondrial production of O_2^- was initiated by direct deformation of the mitochondria, we examined mitochondria in live cells labeled with a mitochondrial specific dye, MitoTracker Orange. Labeled cells were imaged before and during the application of strain. As indicted in Figure 6, mitochondria were observed to distend as the Silastic membrane was strained biaxially by 17%. Measurements made of the total length of selected mitochondria (6 mitochondria from four different fields) increased from 3.1 ± 0.6 μm to 4.1 ± 0.7 μm (32.1% linear strain) indicating local deformation when a global strain was applied. The observed mitochondrial deformation may contribute to initiation of strain-induced O_2^- production.

NADPH oxidase activity is increased by cyclic mechanical strain. We next investigated whether NADPH oxidase contributed to the stretch-induced production of ROS in pulmonary epithelial cells. NADPH oxidase has previously been implicated in the ROS produced by CMS of endothelial cells (3, 24, 29, 48) and VSMC (22, 31). As

shown in Figure 7, cyclic stretch of 16HBE cells significantly increased the activity of NADPH oxidase to 204.8 ± 27.8% relative to un-stretched controls ($p < 0.05$, $n = 6$). Also, the normalized activity of NADPH oxidase was reduced to near background levels when 10 μM DPI was added to the chemilumenescence reaction solution of cell homogenates exposed to either 0 or 2 h of CMS. The chemilumenescence signal was the same as background if cell homogenate was added to the reaction cocktail without NADPH (data not shown).

DISCUSSION

A recent study demonstrated that mechanical ventilation with lower tidal volumes reduced the mortality of ARDS patients (40), and these findings are supported by studies demonstrating that lower tidal volume settings decreased injury to epithelial and endothelial cells in ventilated rats (12) and decreased inflammation in a mouse model of VILI (5, 46). Thus, higher tidal volumes may contribute to VILI through mechanisms related to overdistention of the lungs. We hypothesized that over-distention of the lung epithelium leads to increased production of ROS that may contribute to VILI. We exposed pulmonary epithelial cells to cyclic mechanical strain (CMS) and measured the production of superoxide with dihydroethidium (DHE). We found that O_2^- production was significantly increased after 2 h of CMS of 16HBE, A549, and primary rat AT II cells compared to static controls (see Figure 1B). We examined superoxide production in order to focus our study on the potential initial events stimulated by mechanical stretch.

CMS of A549 cells has been shown previously to increase generation of ROS. Upadhyay et al. demonstrated that A549 cells stretched for 1 h at 30% biaxial elongation and 30 cpm increased generation of hydrogen peroxide (H_2O_2) by 25% as compared to static controls (42). In that study the cells were loaded with 2,7-dichlorodihydrofluorescein (DCFH), which is oxidized to the fluorescent compound dichlorofluorescein (DCF) by H_2O_2. Hydrogen peroxide is one of several downstream metabolites of superoxide generation. We measured a greater increase in ROS production by A549 cells using DHE after 2 h of CMS (Figure 1B). The lower increase in ROS production detected by Upadhyay et al. may be due to the metabolism of superoxide to other pathways not detected by DCFH. In addition, DCFH has been

reported to leak out of cells (37), and in preliminary experiments we too observed leakage of DCFH from cells. Also, stretching cells loaded with this dye may cause further leakage through transient, non-lethal strain-induced membrane breaks (44). Oxidized DHE binds to DNA and fluoresces, and thus the fluorescent dye remains inside the cells. We loaded the dye after the stretch concluded, reducing potential leakage of the DHE dye. Differences between our study and previous studies could also be due to the duration of the stretch. We measured changes in ROS production over time in 16HBE cells (Figure 2), and found that CMS of 0.5 h did not elicit an increase in O_2^- production, but 2 h caused a significant increase. Although we did not measure ROS production after 1 h of CMS in A549 cells, the response may be similar to that reported by Upadhyay et al. (42).

Other investigators have used DHE to monitor changes in O_2^- production in human lung endothelial cells exposed to hyperoxia (35), nutrient deprived human aortic endothelial cells (28), and angiotensin II treatment of bovine aortic endothelial cells (9). Lopez et al. used images of DHE staining to quantify changes in the generation of O_2^- with nutrient deprivation (28). We used a similar method to quantify changes in the current study. Parinandi et al. used cell lysate fluorescence from DHE loaded cells to measure changes in O_2^- production (35). Superoxide production has also been measured by an HPLC method in cells and intact tissues (9) based on the fluorescence of oxoethidium. This study also demonstrated the specificity of DHE for O_2^- by showing that fluorescence was not increased after treatment with H_2O_2, peroxynitrite, or hypochlorous acid.

ROS generation caused by CMS resulted in a significant reduction of the ratio of GSH to GSSG in 16HBE cells indicating an oxidant stress that occurred as early as 0.5 h, and the ratio remained significantly reduced through 24 h (see Figure 3). An increase in ROS production as a result of CMS was not observed in 16HBE cells until 2 h of strain as measured by DHE fluorescence (see Figure 4), but the GSH/GSSG ratio indicated an oxidant stress after only 0.5 h of stretch. This implies that the cellular anti-oxidant defenses were able to absorb the excess ROS before being overwhelmed by 2 h, resulting in an increase in DHE fluorescence. However, after 24 h DHE measurements returned to basal levels while the GSH/GSSG ratio remained significantly reduced. Jafari et al. measured GSH levels in A549 cells and found that levels were significantly reduced after 1 h of CMS at 15% strain and 20 cpm, returned to basal levels after 2 and 3 h, but showed a significant increase after 4 h CMS (23). Our results corroborate their findings of an early oxidant stress caused by CMS. However, in our study while the ratio of GSH/GSSG decreased, GSH levels were maintained at a constant level in 16HBE cells subjected to CMS with no significant changes over 24 h, while total GSH levels increased significantly after 24 h resulting in the continued reduction in the ratio (data not shown). This may not fully explain the reduction in O_2^- after 24 h, but we did not investigate activity or protein levels of anti-oxidants more specific to O_2^- such as superoxide dismutase. Increased levels of superoxide dismutase after 24 hr might account for the decrease in superoxide production with the sustained decrease in GSH/GSSG ratio. Differences between antioxidant systems in 16HBE and A549 cells may also contribute to the observed differences. However, measurement of both GSH and GSSG levels is important to assess the redox state of the cells.

We explored the effects of varying the magnitude of strain on ROS production of pulmonary epithelial cells and found that application of strain levels <15% elongation resulted in superoxide production that was not significantly different from control. Application of strain levels ≥15% caused significant increases in ROS production (Figure 4). To our knowledge, this is the first time ROS production has been studied as a function of the magnitude of strain in pulmonary epithelial cells. These results suggest that a threshold level of strain exists above which elevated ROS production occurs. The strain levels experienced by the lungs *in vivo* during either spontaneous breathing or mechanical ventilation are difficult to determine. Tshumperlin and Margulies (41) measured the changes in epithelial basement membrane surface area (EBMSA) of lungs fixed at different inflations and found the expected non-linear response. Inflation from 24% to total lung capacity (TLC) caused a 40% increase in EBMSA, while inflation from 42% of TLC to TLC resulted in a 34% increase. This change in surface area corresponds to a linear strain of approximately 18%. In injured lungs, some regions may be collapsed or fluid-filled, functionally reducing the volume of the lungs. Therefore, during mechanical ventilation the remaining volume of the lungs may be significantly over-inflated, causing even greater distention and injury (20). However, the actual levels of strain in the airways and alveoli in injured lungs have not been well-characterized. Some authors have suggested that linear strain of ~10% occurs during normal breathing, and that higher levels occur during high tidal volume mechanical ventilation, but there are no direct measurements of this. Our results showed that ROS production was significantly increased at strains of 15% or greater. During mechanical ventilation at high tidal volumes or even during lower tidal volumes if the lung volume is effectively reduced by

injury, the average distention of the tissue may be above this threshold and cause generation of ROS from the epithelium.

In this study we were unable to stretch the primary rat ATII cells at 20% elongation and 30 cycles/min because significant detachment of the cells from the membrane occurred. Therefore, the values reported in Figure 1B for rat ATII cells are from cells stretched at 15% strain and 15 cpm on day 2 of culture, and the cells remained attached under these conditions. Oswari et al. showed a substantial loss of viability (49%) in rat AT II cells cultured for one day on fibronectin-coated Silastic and exposed to 1 h of CMS of 25% change in surface area (~12% linear strain) and 15 cycles/min (33). However, treatment with keratinocyte growth factor or culture of the cells on a matrix deposited by AT II cells for five days resulted in levels of viability similar to static controls. We are currently adapting our culture methods to better promote attachment and survival at increased strain and frequency. Despite the lower strain and frequency of stretch, we observed a significant stimulation of ROS production albeit at a lower level than that seen in the cell lines tested.

The source of mechanical strain- or shear stress-induced ROS is currently debated, and potential sources in different cell types include NADPH oxidase (7, 13, 29, 30), xanthine oxidase (30), NO sythase, and the mitochondria (2, 21). Previous studies with endothelial cells concluded that the source of ROS was primarily NADPH oxidase since treatment with the flavoprotein inhibitor, DPI, abolished the response. However, DPI is a non-specific inhibitor of NADPH oxidase that also inhibits other potential sources of ROS generation including the enzymes of the electron transport chain in mitochondria. Recent studies have demonstrated that mitochondria are involved in

strain-induced production of ROS in endothelial cells. Ichimura et al. (21) and Ali et al. (2) have shown that the Complex I inhibitor, rotenone, eliminated strain-induced ROS production. Ali et al. also used ethidium-treated HUVEC cultures to eliminate mitochondrial DNA and the electron transport chain proteins and found that the CMS-induced increase in ROS production was eliminated. A more specific pharmacological inhibitor of NADPH oxidase, apocynin, was employed and was found to have no effect on CMS-induce ROS generation. We found that CMS of 16HBE cells stimulated NADPH oxidase activity and that ROS production was partially sensitive to inhibition of mitochondrial Complex I. The activity of NADPH oxidase, measured by Lucigenin chemilumenescence, increased significantly after 2 h of CMS (Figure 6). Treatment of the cell lysates with DPI (10 μM) inhibited the increase in activity, and reduced the activity in static cell lysates to similar levels. The specificity of the response was tested by comparing results with and without an excess of NADPH (50 μM) in the reaction mixture. Chemilumenescent readings were similar to background when NADPH was not included in the reaction cocktail (data not shown). Rotenone partially inhibited CMS-induced increases in DHE fluorescence (Figure 5). Taken together, our results suggest that CMS-induced increases in ROS production are due to both NADPH oxidase and mitochondrial generation in pulmonary epithelial cells.

If mitochondrial production of superoxide is stimulated by mechanical stretch, then what is the initiating event? We hypothesized that global strain applied to the cells may lead to direct distention of the mitochondria, since mitochondria are attached to both the actin (39) and microtubule (16, 17) components of the cytoskeleton. We observed substantial deformation of mitochondrial structures when cells were stretched (Figure 7).

We speculate that mechanical distention of mitochondrial structures may activate pathways that lead to generation of ROS. For example, mitochondrial K^+_{ATP} activation has been linked to generation of ROS (11, 15), and activation of the mitochondrial ATP-sensitive K^+ (K^+_{ATP}) channel has been linked to mitochondrial swelling (18). However, the mechanism of ROS production through activation of the mitochondrial K^+_{ATP} channel has not been determined, and no studies have connected the distention caused by mitochondrial swelling to ROS production. One of the major limitations of our measurements of mitochondrial deformation is that the images that were analyzed (Figure 6) were from a single plane of focus. Because we did not collect images at different z-planes, we can not exclude the possibility that the change in length that was observed was due to the appearance of mitochondrial structures from out of focus planes in the images of stretched cells. However, these images were not taken with a confocal microscope, and thus contributions from multiple planes are more likely to appear in the image. In addition, 16HBE cells are quite thin, and we specifically identified mitochondrial structures that were in more confined areas near the cell boarder or beneath the nucleus making the possibility of out of plane regions appearing in the focal plane less likely. These considerations, however, still do not rule out the possibility that apparent deformation was due to the appearance of out of focus structures.

One proposed mechanism for VILI is that increased mechanical deformation of lung tissue stimulates an acute inflammatory response characterized by increased levels of pro-inflammatory cytokines and inflammatory cell infiltration. In previous studies high tidal volume mechanical ventilation without underlying lung injury led to both increased cytokine production (46) and enhanced neutrophil infiltration (5). CMS has

been shown to stimulate production of pro-inflammatory cytokines in both airway and alveolar cells. CMS of BEAS-2B, an airway epithelial cell line, resulted in an increased production of interleukin-8 (IL 8) (34). A549 cells when subjected to CMS increased production of pro-inflammatory cytokines IL 8 (23, 27, 43, 49), IL 6 (23), and transforming growth factor β (49). Primary cultures of rat AT II also exhibited CMS-induced production of IL 8 (36). Exposure to H_2O_2 or exogenous O_2^- production by xanthine/xanthine oxidase and exposure of rat AT II cells to hyperoxia also caused increased production of the pro-inflammatory cytokines IL 1β, IL 6, and TNF-α (14). Ali et al. demonstrated that stretch-induced expression of VCAM-1 and activation of NF-κB could be abrogated by blocking mitochondrial generation of ROS in endothelial cells (2). Thus, inflammatory responses may be initiated by stretch-induced production of ROS. We demonstrated in this study that stretch stimulated increased ROS production in both airway and alveolar epithelial cells, that the response was both time-varying and magnitude-dependent, and that ROS are derived from both NADPH oxidase and mitochondria.

ACKNOWLEDGMENTS

We gratefully acknowledge Dr. Harry Ischiropoulos and Dr. Navdeep Chandel for helpful discussions regarding this study, and Dr. Karen Ridge for discussions regarding type II cell isolations. We also thank Charlean Luellen for expert technical assistance. This work was supported by NIH grants HL064981, HL004479, HL63886, and HL72902.

FIGURE LEGENDS

Figure 1: Cyclic mechanical stretch (CMS) caused increased O_2^- production in pulmonary epithelial cells. A) Sample images of DHE staining of static 16HBE cells and 16HBE cells stretched for 2 h (bar = 15 μm). The grey scale for display was matched for the two images. B) DHE fluorescence values were measured after 2 h of CMS and normalized to the respective unstretched control for 16HBE (open bars), AT II (striped bars), and A549 (solid bars) cells (n = 7, 6, and 3 respectively). * represents a significantly different value in normalized fluorescence compared to static controls ($p < 0.05$).

Figure 2: Time course of O_2^- production in response to stretch. 16HBE cells were stretched for 0, 0.5, 2, 6, 12, 18, or 24 h (n = 24, 9, 7, 9, 9, 9, and 9, respectively) at 20% strain and 30 cpm and then stained with DHE. Values presented are normalized to the unstretched (0 h) control values for each experiment. * represents a significantly different value in normalized fluorescence compared to static controls ($p < 0.05$).

Figure 3: GSH oxidation increased in 16HBE after CMS. The GSH/GSSG ratio was determined after 0, 0.5, 2, 6, 12, or 24 h (n = 6, 4, 4, 4, 4, and 4, respectively) of stretch at 20% strain and 30 cpm. Values presented are normalized to the unstretched (0 h) control values for each experiment. * represents a significantly different value in normalized fluorescence compared to static controls ($p < 0.05$).

Figure 4: Superoxide production was dependent upon the magnitude of strain in 16HBE cells. Cells were stretched 0, 10, 15, 20, or 30 % for 2 h (n = 12, 6, 6, 6, and 6, respectively) at 30 cpm. The DHE fluorescence was measured and normalized to the unstretched control for each experiment. * represents a significantly different value in normalized fluorescence compared to static controls ($p < 0.05$). There was no significant difference between the 15%, 20%, and 30% stretch groups compared with one another.

Figure 5: Rotenone partially inhibited the CMS-induced increase in O_2^- production. Rotenone (25 nM) (n = 9), vehicle (n = 3), or no treatment (n = 9) was applied during the 2 h of stretch at 20% strain and 30 cpm. Values presented are normalized to the unstretched control. * represents a significantly different value in normalized fluorescence compared to static controls ($p < 0.05$). # represents a significantly different value in normalized fluorescence compared to the 2 h of stretch with no treatment ($p < 0.05$).

Figure 6: Mechanical strain deforms mitochondria of 16HBE cells. Mitochondria were labeled using MitoTracker Orange. The white bar represents a distance of 30 μm in the original images. The black bar represents a span of 3 μm in the zoomed fields.

Figure 7: CMS increased NADPH oxidase activity in 16HBE cells. Cells were strained for 0 or 2 h at 20% and 30 cpm. DPI was included in the chemiluminescence reaction buffer at a concentration of 0 μM (open bars; n = 5 and 6 respectively) or 10 μM (solid

bars; n = 3 and 1 respectively). * represents a significantly different value in normalized chemiluminescence compared to static controls ($p < 0.05$).

REFERENCES

1. Aikawa R, Nagai T, Tanaka M, Zou Y, Ishihara T, Takano H, Hasegawa H, Akazawa H, Mizukami M, Nagai R and Komuro I. Reactive oxygen species in mechanical stress-induced cardiac hypertrophy. *Biochem Biophys Res Commun* 289: 901-907., 2001.

2. Ali MH, Pearlstein DP, Mathieu CE and Schumacker PT. Mitochondrial requirement for endothelial responses to cyclic strain: implications for mechanotransduction. *Am J Physiol Lung Cell Mol Physiol* 287: L486-496, 2004.

3. Cheng J-J, Chao Y-J and Wang DL. Cyclic Strain Activates Redox-sensitive Proline-rich Tyrosine Kinase 2 (PYK2) in Endothelial Cells. *J. Biol. Chem.* 277: 48152-48157, 2002.

4. Chiu JJ, Wung BS, Shyy JYJ, Hsieh HJ and Wang DL. Reactive Oxygen Species Are Involved in Shear Stress-Induced Intercellular Adhesion Molecule-1 Expression in Endothelial Cells. *Arterioscler Thromb Vasc Biol* 17: 3570-3577, 1997.

5. Choudhury S, Wilson MR, Goddard ME, O'Dea KP and Takata M. Mechanisms of early pulmonary neutrophil sequestration in ventilator-induced lung injury in mice. *Am J Physiol Lung Cell Mol Physiol* 287: L902-910, 2004.

6. D'Angio CT, LoMonaco MB, Johnston CJ, Reed CK and Finkelstein JN. Differential roles for NF-kappa B in endotoxin and oxygen induction of interleukin-8 in the macrophage. *American Journal of Physiology - Lung Cellular & Molecular Physiology* 286: L30-36, 2004.

7. De Keulenaer GW, Chappell DC, Ishizaka N, Nerem RM, Alexander RW and Griendling KK. Oscillatory and steady laminar shear stress differentially affect

human endothelial redox state: role of a superoxide-producing NADH oxidase. ***Circ Res*** **82: 1094-1101, 1998.**

8. Dobbs LG. Isolation and culture of alveolar type II cells. ***Am J Physiol*** **258: L134-147, 1990.**

9. Fink B, Laude K, McCann L, Doughan A, Harrison DG and Dikalov S. Detection of intracellular superoxide formation in endothelial cells and intact tissues using dihydroethidium and an HPLC-based assay. ***Am J Physiol Cell Physiol*** **287: C895-902, 2004.**

10. Fisher JL, Levitan I and Margulies SS. Plasma Membrane Surface Increases with Tonic Stretch of Alveolar Epithelial Cells. ***Am. J. Respir. Cell Mol. Biol.*****: 2003-0224OC, 2004.**

11. Forbes RA, Steenbergen C and Murphy E. Diazoxide-Induced Cardioprotection Requires Signaling Through a Redox-Sensitive Mechanism. ***Circ Res*** **88: 802-809, 2001.**

12. Frank JA, Gutierrez JA, Jones KD, Allen L, Dobbs L and Matthay MA. Low Tidal Volume Reduces Epithelial and Endothelial Injury in Acid-injured Rat Lungs. ***Am. J. Respir. Crit. Care Med.*** **165: 242-249, 2002.**

13. Grote K, Flach I, Luchtefeld M, Akin E, Holland SM, Drexler H and Schieffer B. Mechanical Stretch Enhances mRNA Expression and Proenzyme Release of Matrix Metalloproteinase-2 (MMP-2) via NAD(P)H Oxidase-Derived Reactive Oxygen Species. ***Circ Res*** **92: 80e-86, 2003.**

14. Haddad JJ. Redox regulation of pro-inflammatory cytokines and IkappaB-alpha/NF-kappaB nuclear translocation and activation. ***Biochem Biophys Res Commun*** **296: 847-856., 2002.**

15. Han J, Kim N, Park J, Seog DH, Joo H and Kim E. Opening of mitochondrial ATP-sensitive potassium channels evokes oxygen radical generation in rabbit heart slices. ***J Biochem (Tokyo)*** **131: 721-727., 2002.**

16. Heggeness MH, Simon M and Singer SJ. Association of mitochondria with microtubules in cultured cells. ***Proc Natl Acad Sci U S A*** **75: 3863-3866, 1978.**

17. Hirokawa N. Kinesin and dynein superfamily proteins and the mechanism of organelle transport. ***Science*** **279: 519-526, 1998.**

18. Holmuhamedov EL, Jovanovic S, Dzeja PP, Jovanovic A and Terzic A. Mitochondrial ATP-sensitive K+ channels modulate cardiac mitochondrial function. ***Am J Physiol Heart Circ Physiol*** **275: H1567-1576, 1998.**

19. Hsieh HJ, Cheng CC, Wu ST, Chiu JJ, Wung BS and Wang DL. Increase of reactive oxygen species (ROS) in endothelial cells by shear flow and involvement of ROS in shear-induced c-fos expression. ***J Cell Physiol*** **175: 156-162., 1998.**

20. Hubmayr RD. Perspective on Lung Injury and Recruitment: A Skeptical Look at the Opening and Collapse Story. ***Am. J. Respir. Crit. Care Med.*** **165: 1647-1653, 2002.**

21. Ichimura H, Parthasarathi K, Quadri S, Issekutz AC and Bhattacharya J. Mechano-oxidative coupling by mitochondria induces proinflammatory responses in lung venular capillaries. ***J. Clin. Invest.*** **111: 691-699, 2003.**

22. Inoue N, Kawashima S, Hirata K-I, Rikitake Y, Takeshita S, Yamochi W, Akita H and Yokoyama M. Stretch force on vascular smooth muscle cells enhances oxidation of LDL via superoxide production. ***Am J Physiol Heart Circ Physiol*** **274: H1928-1932, 1998.**

23. Jafari B, Ouyang B, Li LF, Hales CA and Quinn DA. Intracellular glutathione in stretch-induced cytokine release from alveolar type-2 like cells. ***Respirology*** **9: 43-53., 2004.**

24. Juan SH, Chen JJ, Chen CH, Lin H, Cheng CF, Liu JC, Hsieh MH, Chen YL, Chao HH, Chen TH, Chan P and Cheng TH. 17beta-estradiol inhibits cyclic strain-induced endothelin-1 gene expression within vascular endothelial cells. ***Am J Physiol Heart Circ Physiol*** **287: H1254-1261, 2004.**

25. Kamencic H, Lyon A, Paterson PG and Juurlink BHJ. Monochlorobimane Fluorometric Method to Measure Tissue Glutathione*1. ***Analytical Biochemistry*** **286: 35-37, 2000.**

26. Kheradmand F, Folkesson HG, Shum L, Derynk R, Pytela R and Matthay MA. Transforming growth factor-alpha enhances alveolar epithelial cell repair in a new in vitro model. ***American Journal of Physiology*** **267: L728-738, 1994.**

27. Li L-F, Ouyang B, Choukroun G, Matyal R, Mascarenhas M, Jafari B, Bonventre JV, Force T and Quinn DA. Stretch-induced IL-8 depends on c-Jun NH2-terminal and nuclear factor-{kappa}B-inducing kinases. ***Am J Physiol Lung Cell Mol Physiol*** **285: L464-475, 2003.**

28. Lopes NHM, Vasudevan SS, Gregg D, Selvakumar B, Pagano PJ, Kovacic H and Goldschmidt-Clermont PJ. Rac-Dependent Monocyte Chemoattractant Protein-1 Production Is Induced by Nutrient Deprivation. ***Circ Res*** **91: 798-805, 2002.**

29. Matsushita H, Lee Kh K and Tsao PS. Cyclic strain induces reactive oxygen species production via an endothelial NAD(P)H oxidase. ***J Cell Biochem*** **81: 99-106, 2001.**

30. McNally JS, Davis ME, Giddens DP, Saha A, Hwang J, Dikalov S, Jo H and Harrison DG. Role of Xanthine Oxidoreductase and the NAD(P)H oxidase in Endothelial Superoxide Production in Response to Oscillatory Shear Stress. ***Am J Physiol Heart Circ Physiol*** **4: 4, 2003.**

31. Nguyen KT, Frye SR, Eskin SG, Patterson C, Runge MS and McIntire LV. Cyclic Strain Increases Protease-Activated Receptor-1 Expression in Vascular Smooth Muscle Cells. ***Hypertension*** **38: 1038-1043, 2001.**

32. Olivera W, Ridge K, Wood LD and Sznajder JI. Active sodium transport and alveolar epithelial Na-K-ATPase increase during subacute hyperoxia in rats. ***Am J Physiol*** **266: L577-584, 1994.**

33. Oswari J, Matthay MA and Margulies SS. Keratinocyte growth factor reduces alveolar epithelial susceptibility to in vitro mechanical deformation. ***Am J Physiol Lung Cell Mol Physiol*** **281: L1068-1077, 2001.**

34. Oudin S and Pugin J. Role of MAP Kinase Activation in Interleukin-8 Production by Human BEAS-2B Bronchial Epithelial Cells Submitted to Cyclic Stretch. ***Am. J. Respir. Cell Mol. Biol.*** **27: 107-114, 2002.**

35. Parinandi NL, Kleinberg MA, Usatyuk PV, Cummings RJ, Pennathur A, Cardounel AJ, Zweier JL, Garcia JGN and Natarajan V. Hyperoxia-induced NAD(P)H oxidase activation and regulation by MAP kinases in human lung endothelial cells. *Am J Physiol Lung Cell Mol Physiol* 284: L26-38, 2003.

36. Quinn D, Tager A, Joseph PM, Bonventre JV, Force T and Hales CA. Stretch-Induced Mitogen-Activated Protein Kinase Activation and Interleukin-8 Production in Type II Alveolar Cells. *Chest* 116: 89S-90, 1999.

37. Royall JA and Ischiropoulos H. Evaluation of 2',7'-dichlorofluorescin and dihydrorhodamine 123 as fluorescent probes for intracellular H2O2 in cultured endothelial cells. *Arch Biochem Biophys* 302: 348-355, 1993.

38. Savla U and Waters CM. Mechanical strain inhibits repair of airway epithelium in vitro. *American Journal of Physiology* 274: L883-892, 1998.

39. Starr DA and Han M. Role of ANC-1 in Tethering Nuclei to the Actin Cytoskeleton. *Science* 298: 406-409, 2002.

40. The Acute Respiratory Distress Syndrome Network. Ventilation with Lower Tidal Volumes as Compared with Traditional Tidal Volumes for Acute Lung Injury and the Acute Respiratory Distress Syndrome. *N Engl J Med* 342: 1301-1308, 2000.

41. Tschumperlin DJ and Margulies SS. Alveolar epithelial surface area-volume relationship in isolated rat lungs. *J Appl Physiol* 86: 2026-2033, 1999.

42. Upadhyay D, Correa-Meyer E, Sznajder JI and Kamp DW. FGF-10 prevents mechanical stretch-induced alveolar epithelial cell DNA damage via MAPK activation. *Am J Physiol Lung Cell Mol Physiol* 284: L350-359, 2003.

43. Vlahakis NE, Schroeder MA, Limper AH and Hubmayr RD. Stretch induces cytokine release by alveolar epithelial cells in vitro. ***Am J Physiol Lung Cell Mol Physiol*** **277: L167-173, 1999.**

44. Vlahakis NE, Schroeder MA, Pagano RE and Hubmayr RD. Deformation-induced lipid trafficking in alveolar epithelial cells. ***Am J Physiol Lung Cell Mol Physiol*** **280: L938-946, 2001.**

45. Wei Z, Costa K, Al-Mehdi AB, Dodia C, Muzykantov V and Fisher AB. Simulated ischemia in flow-adapted endothelial cells leads to generation of reactive oxygen species and cell signaling. ***Circ Res*** **85: 682-689, 1999.**

46. Wilson MR, Choudhury S, Goddard ME, O'Dea KP, Nicholson AG and Takata M. High tidal volume upregulates intrapulmonary cytokines in an in vivo mouse model of ventilator-induced lung injury. ***J Appl Physiol*** **95: 1385-1393, 2003.**

47. Wung BS, Cheng JJ, Hsieh HJ, Shyy YJ and Wang DL. Cyclic strain-induced monocyte chemotactic protein-1 gene expression in endothelial cells involves reactive oxygen species activation of activator protein 1. ***Circ Res*** **81: 1-7., 1997.**

48. Wung BS, Cheng JJ, Shyue S-K and Wang DL. NO Modulates Monocyte Chemotactic Protein-1 Expression in Endothelial Cells Under Cyclic Strain. ***Arterioscler Thromb Vasc Biol*** **21: 1941-1947, 2001.**

49. Yamamoto H, Teramoto H, Uetani K, Igawa K and Shimizu E. Cyclic stretch upregulates interleukin-8 and transforming growth factor-beta1 production through a protein kinase C-dependent pathway in alveolar epithelial cells. ***Respirology*** **7: 103-109, 2002.**

50. Yeh LH, Park YJ, Hansalia RJ, Ahmed IS, Deshpande SS, Goldschmidt-Clermont PJ, Irani K and Alevriadou BR. Shear-induced tyrosine phosphorylation in endothelial cells requires Rac1-dependent production of ROS. ***Am J Physiol*** **276: C838-847., 1999.**

51. Zhuang D, Ceacareanu AC, Lin Y, Ceacareanu B, Dixit M, Chapman KE, Waters CM, Rao GN and Hassid A. Nitric oxide attenuates insulin- or IGF-I-stimulated aortic smooth muscle cell motility by decreasing H2O2 levels: essential role of cGMP. ***Am J Physiol Heart Circ Physiol*** **286: H2103-2112, 2004.**

Figure 1

A

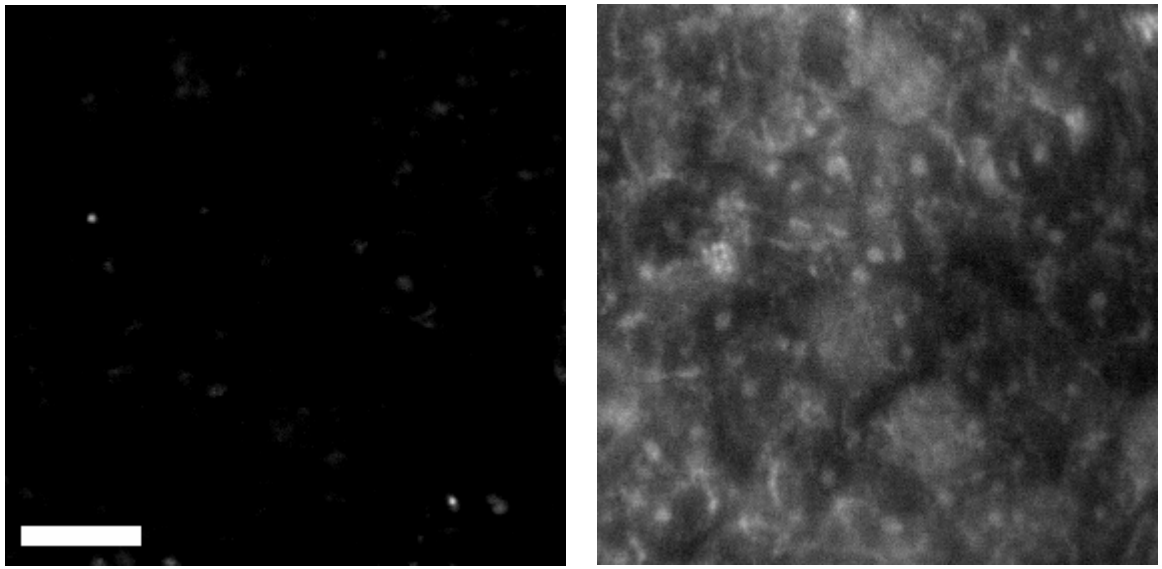

0 h of Stretch

2 h of Stretch

Figure 1

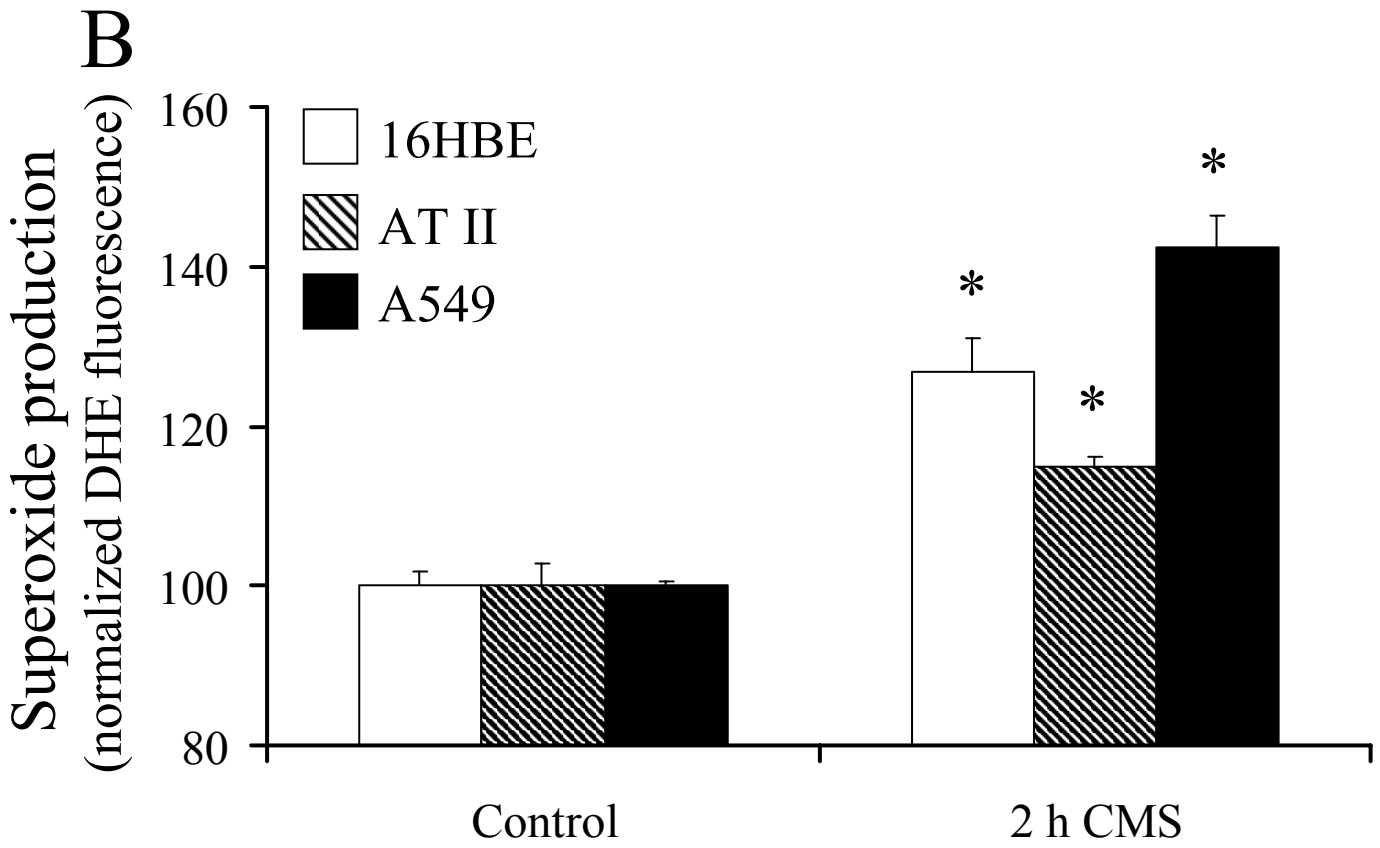
B
Superoxide production
(normalized DHE fluorescence)
160
140
120
100
80
16HBE
AT II
A549
*
*
*
Control
2 h CMS

Figure 2

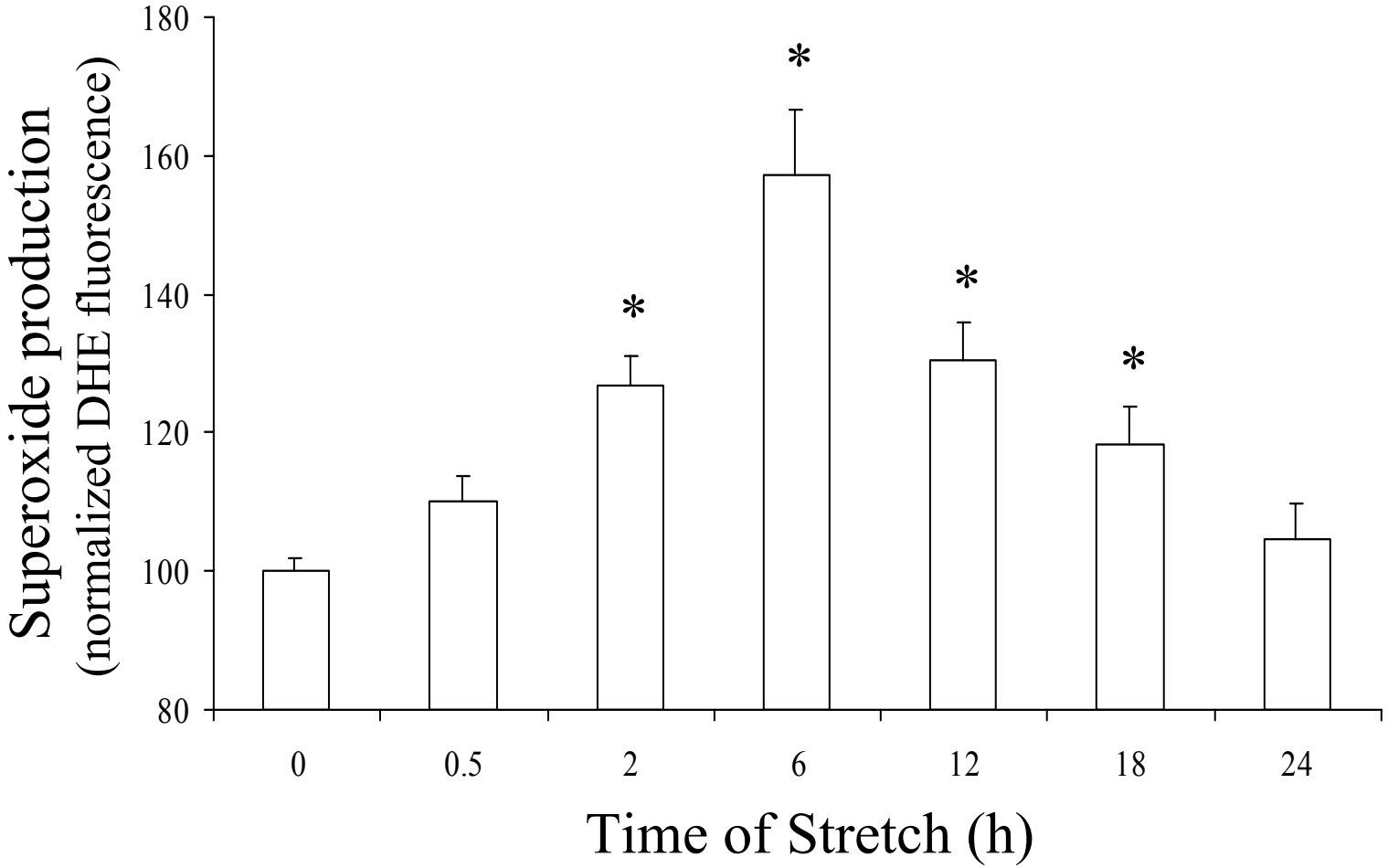
Superoxide production
(normalized DHE fluorescence)
180
160
140
120
100
80
*
*
*
*
0
0.5
2
6
12
18
24
Time of Stretch (h)

Figure 3

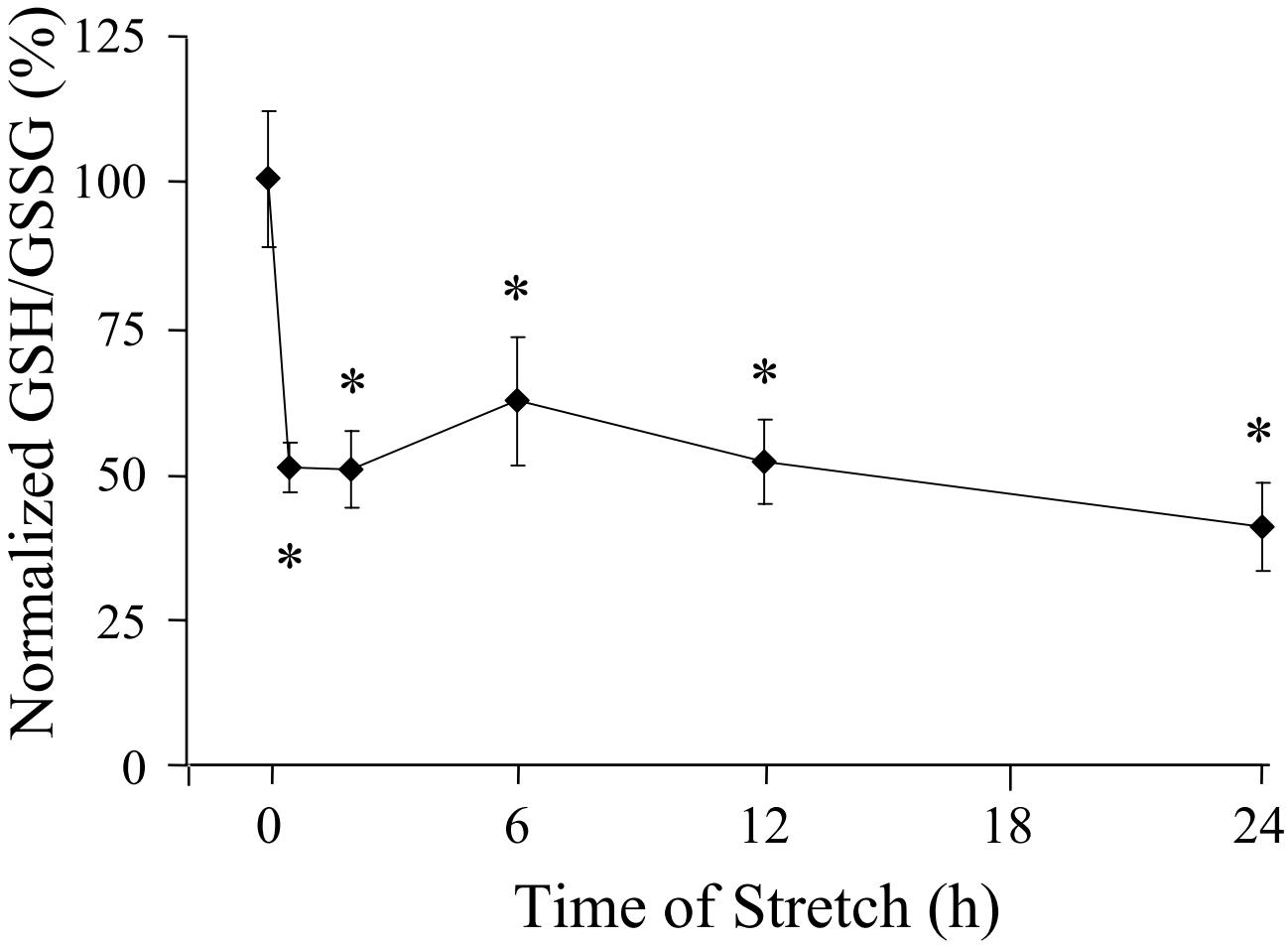
Normalized GSH/GSSG (%)
125
100
75
50
25
0
0
6
12
18
24
Time of Stretch (h)
*
*
*
*
*

Figure 4

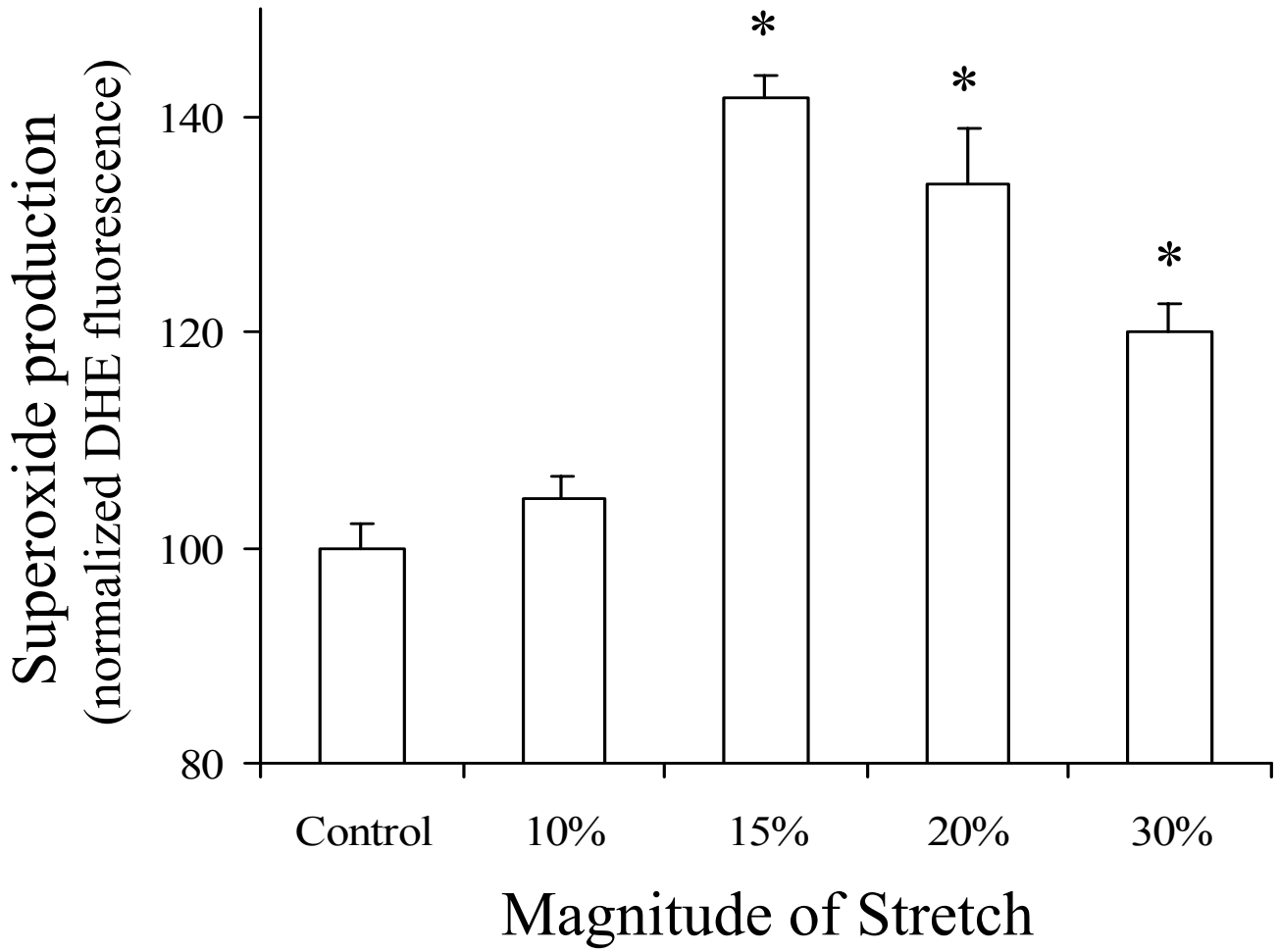
Superoxide production
(normalized DHE fluorescence)
140
120
100
80
*
*
*
Control
10%
15%
20%
30%
Magnitude of Stretch

Figure 5

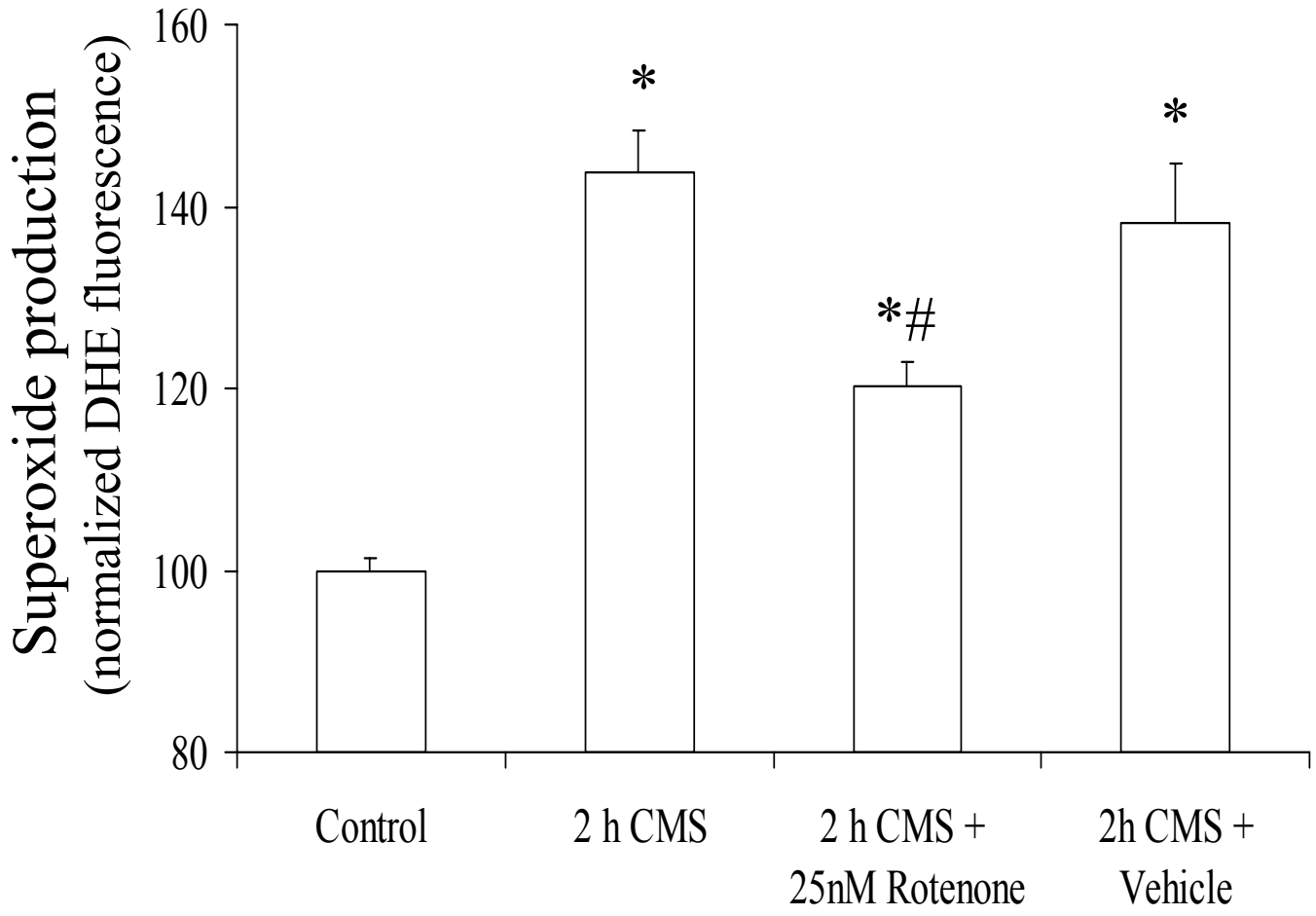
Superoxide production
(normalized DHE fluorescence)
160
140
120
100
80
*
*#
*
Control
2 h CMS
2 h CMS +
25nM Rotenone
2h CMS +
Vehicle

Figure 6

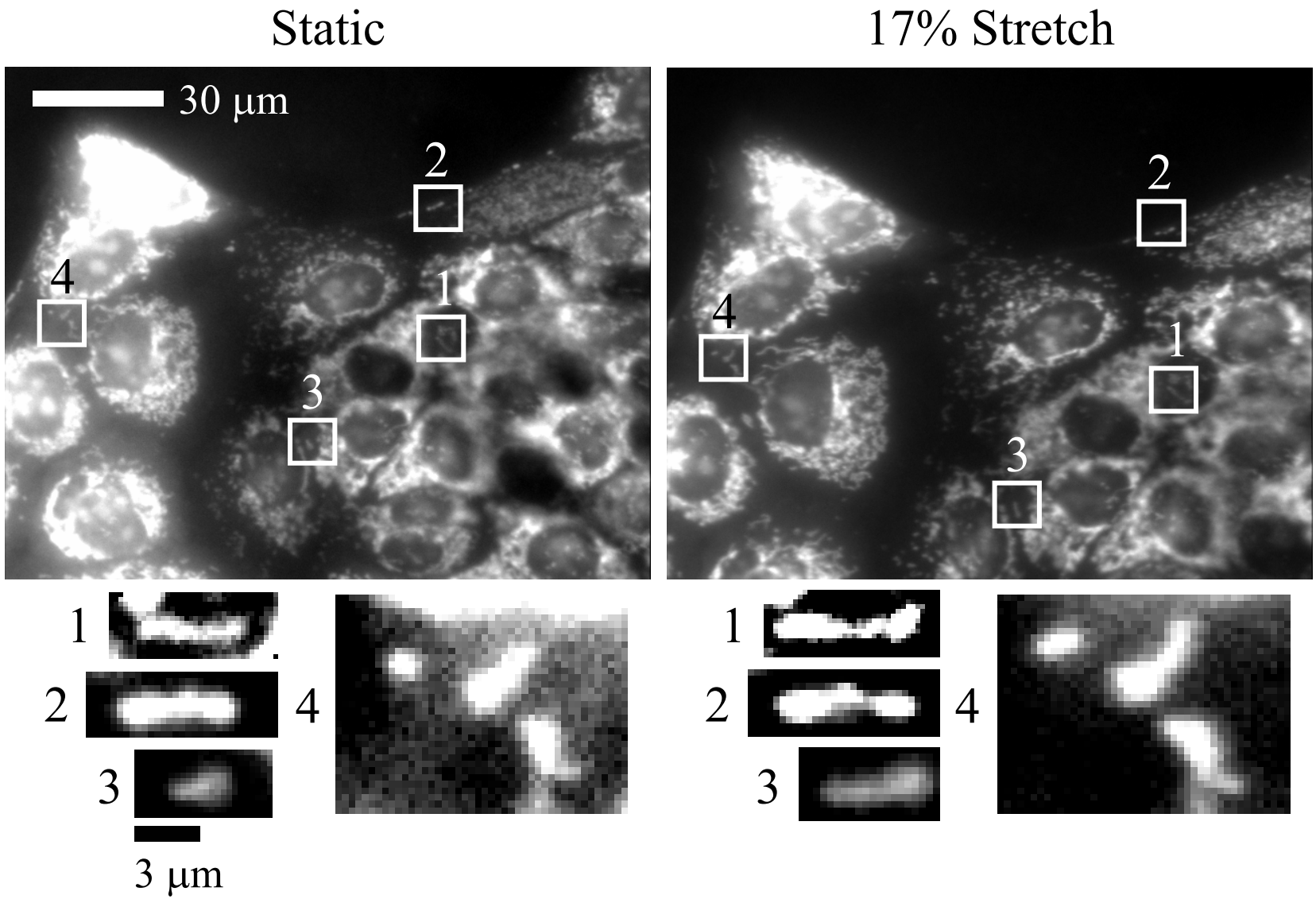

Figure 7

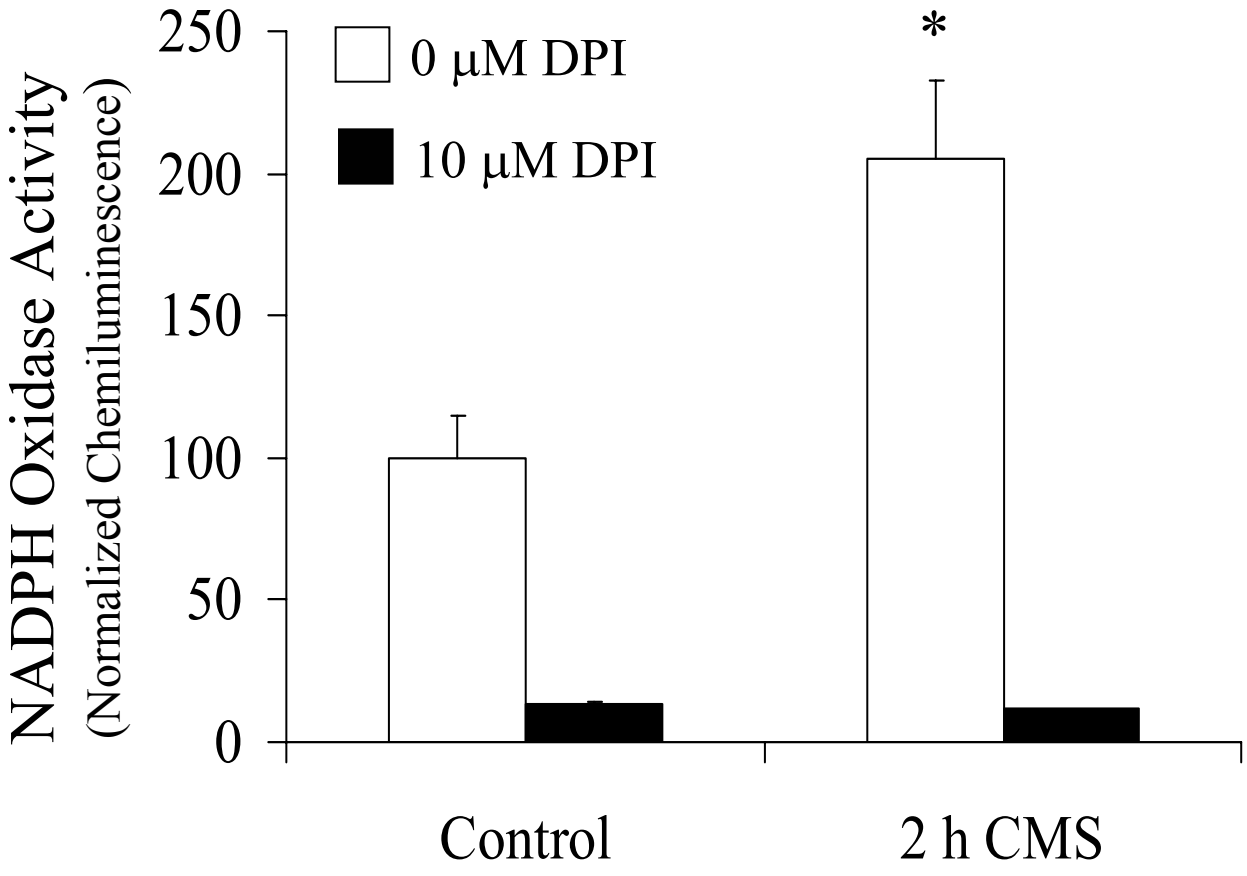
NADPH Oxidase Activity
(Normalized Chemiluminescence)
250
200
150
100
50
0
0 μM DPI
10 μM DPI
*
Control
2 h CMS